Journal of Zhejiang University-SCIENCE A (Applied Physics & Engineering)
ISSN 1673-565X (Print); ISSN 1862-1775 (Online)
www.zju.edu.cn/jzus; www.springerlink.com
E-mail: jzus@zju.edu.cn

# Geotechnical centrifuge model tests for explosion cratering and propagation laws of blast wave in sand*

Yi-kai FAN†[1,2], Zu-yu CHEN[1], Xiang-qian LIANG[1], Xue-dong ZHANG[1], Xin HUANG[2]

([1]*State Key Laboratory of Simulation and Regulation of Water Cycle in River Basin, China Institute of Water Resources and Hydropower Research, Beijing 100044, China*)

([2]*School of Transportation Science and Engineering, Beihang University, Beijing 100191, China*)

†E-mail: yk_fan2006@163.com

Received Sept. 19, 2011; Revision accepted Nov. 21, 2011; Crosschecked Feb. 27, 2012

**Abstract:** This paper presents the explosion cratering effects and their propagation laws of blast waves in dry standard sands using a 450 *g*-t geotechnical centrifuge apparatus. Ten centrifuge model tests were completed with various ranges of explosive mass, burial depth and centrifuge accelerations. Eleven accelerometers were installed to record the acceleration response in sand. The dimensions of the explosion craters were measured after the tests. The results demonstrated that the relationship between the dimensionless parameters of cratering efficiency and gravity scaled yield is a power regression function. Three specific function equations were obtained. The results are in general agreement with those obtained by other studies. A scaling law based on the combination of the $\pi$ terms was used to fit the results of the ten model tests with a correlation coefficient of 0.931. The relationship can be conveniently used to predict the cratering effects in sand. The results also showed that the peak acceleration is a power increasing function of the acceleration level. An empirical exponent relation between the proportional peak acceleration and distance is proposed. The propagation velocity of blast waves is found to be ranged between 200 and 714 m/s.

**Key words:** Centrifuge model tests, Explosion, Craters, Blast waves, Sand
**doi:**10.1631/jzus.A1100227 **Document code:** A **CLC number:** TU411

## 1 Introduction

The geotechnical centrifuge model test, which has been widely used in the past 80 years (Craig, 1989; Taylor, 1995), especially in Russia (the former Soviet Union), UK and USA, provides inertial forces by rotating the model at a high acceleration level, thus producing a stress field in a small-scale model corresponding to that in a prototype. For a centrifuge dynamic test, a small model at *Ng* (*N* times acceleration of earth's gravity) with energy *E* is similar to a large event at *g* with energy equal to $N^3E$ (Schmidt and Holsapple, 1980). It means an experiment with 1 g of explosives at 100*g* can be used to simulate an experiment with 1 t in the field. Pokrovsky and Fyodorov (1965; 1969) studied the effects of buried explosives used in the construction industry by centrifuge tests. In the 1930s, a dry sand and a moist clay were used. The results of the apparent crater were compared to those in the field. Holsapple and Schmidt (1979; 1987), Piekutowski (1980), Housen *et al.* (1983), Schmidt and Housen (1987), and Housen and Holsapple (2003; 2011) introduced "point-source" approximations for the impactor and explosive. A coupling parameter, *C*, was proposed to describe the impactor or explosive. The volume, shape of crater, and cratering time can be derived by this coefficient by dimensional analysis. Lin *et al.* (1994) conducted model tests with small charges, various ranges of burial depths and centrifuge acceleration levels in a lunar soil. The results indicated that there was an

* Project supported by the National Natural Science Foundation of China (No. 50779073), and the Program Foundation of the China Institute of Water Resources and Hydropower Research (IWHR) (No. YANJI ZD0710)

optimum depth of burial of eight charge diameters for obtaining the maximum apparent crater volumes. Simpson *et al*. (2005) investigated explosive cratering on earth-filled embankment dams by geotechnical centrifuge model tests. The explosives were placed and detonated on the surface of the dam crest. The reference values of explosive charges that resulted in dam break were evaluated based on experimental results. Ma *et al.* (2010) carried out centrifuge model tests for responses of shallow-buried circular structures under surface blasting. These tests were completed at a single acceleration level by using the Tsinghua University 50 *g*-t geotechnical centrifuge. Compared with the field tests, centrifuge model tests are advantageous in their high efficiency, security, repeatability, and low cost.

A centrifuge modeling test system for explosion was developed on the China Institute of Water Resources and Hydropower Research (IWHR) geotechnical centrifuge apparatus. Ten model tests for buried explosion in standard sand with varying explosive charges, depths of burst and acceleration levels were completed. Both explosion cratering and propagation laws of blast wave in sand were investigated. Finally, the results and main findings of these tests were summarized.

## 2 Experimental

### 2.1 Equipment and materials

The IWHR geotechnical centrifuge apparatus has a design capacity of 450 *g*-t, a maximum model acceleration of 200*g* in dynamic tests and a maximum payload mass of 1500 kg.

The model container is a thick-walled round steel bucket with internal dimensions of Φ700 mm ×700 mm as shown in Fig. 1. A JMK F3.6 mm camera was used to monitor the sand motions.

The standard sand used in these tests was produced in Pingtan County, Fujian Province of China. It is processed in accordance with the industry standards of China, JTJ051-93 and JTJ059-95. Table 1 lists the grain size distribution of the sand. The water content of the tested sand is close to 0.

The No. 8 detonator caps were used as explosive sources. One cap is equal to 1 g of hexogen explosives (RDX).

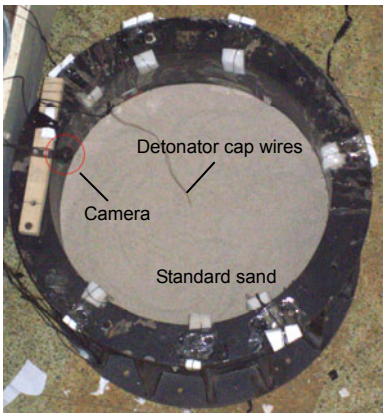


**Fig. 1 Test model with explosive and camera**

**Table 1 Grain size distribution of the sand**

| Grain size (mm) | Finer percentage (%) |
|---|---|
| 1 | 100 |
| 0.5 | 50.5 |
| 0.25 | 13 |
| 0.1 | 0.5 |

### 2.2 Experimental arrangement

Ten centrifuge model tests were completed with various ranges of explosive mass, burial depth and centrifuge accelerations as listed in Table 2. Test GE is completed on ground, and Test CE-*x* (*x*=1,2,…,9) are completed using centrifuge apparatus. The main features of the ten tests involving two groups of explosive charges of 1 and 3 g. The explosives were buried 100 and 150 mm deep from the surfaces of the sand fills that had total heights of 450 and 500 mm, respectively. The locations of the explosives, as well as those of the surrounding accelerators, in reference to the container kept unchanged, are shown in Fig. 2a. These two cases required 273 and 298 kg sand, respectively. Consequently, there are two values of sand density, namely, $1.58\times10^3$ and $1.46\times10^3$ kg/m$^3$. The explosives were detonated at the corresponding acceleration levels.

Eleven accelerometers were installed in the sand to monitor the blast waves. The locations of the accelerometers are shown in Fig. 2 (Fan *et al*., 2012), and the detailed coordinates of the accelerometers are shown in Table 3.

**Table 2 Main features of the tests**

| Test No. | $\rho$ (kg/m$^3$) | $W$ (g) | Depth of burial (mm) | Acceleration level ($\times g$) |
|---|---|---|---|---|
| GE | $1.58\times10^3$ | 1 | 100 | 1 |
| CE-1 | $1.58\times10^3$ | 1 | 100 | 40 |
| CE-2 | $1.58\times10^3$ | 1 | 100 | 70 |
| CE-3 | $1.58\times10^3$ | 1 | 100 | 100 |
| CE-4 | $1.58\times10^3$ | 3 | 100 | 40 |
| CE-5 | $1.58\times10^3$ | 3 | 100 | 70 |
| CE-6 | $1.58\times10^3$ | 3 | 100 | 100 |
| CE-7 | $1.46\times10^3$ | 3 | 150 | 40 |
| CE-8 | $1.46\times10^3$ | 3 | 150 | 70 |
| CE-9 | $1.46\times10^3$ | 3 | 150 | 100 |

$W$: charge mass; $\rho$: sand density

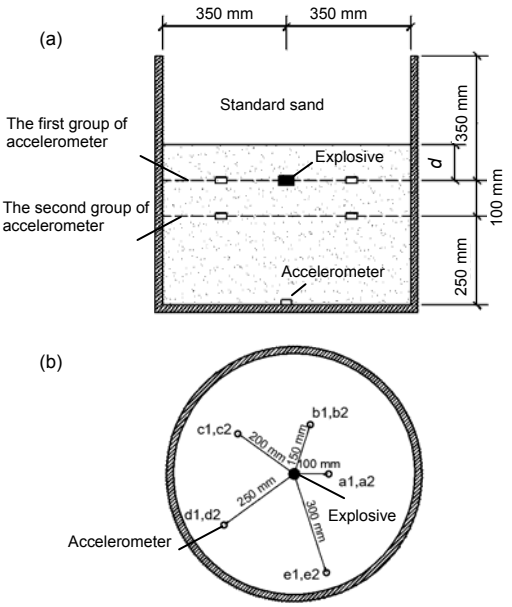


**Fig. 2 Layout of experiment (Fan *et al*., 2012)**
(a) Profile of the test model; (b) Arrangement of accelerometers in the first and the second groups

**Table 3 Coordinates of the accelerometers**

| No. | Distance from the explosive | | |
|---|---|---|---|
| | Horizontal (mm) | Vertical (mm) | Straight line (mm) |
| a1 | 100 | 0 | 100.0 |
| b1 | 150 | 0 | 150.0 |
| c1 | 200 | 0 | 200.0 |
| d1 | 250 | 0 | 250.0 |
| e1 | 300 | 0 | 300.0 |
| a2 | 100 | 100 | 141.4 |
| b2 | 150 | 100 | 180.3 |
| c2 | 200 | 100 | 223.6 |
| d2 | 250 | 100 | 269.3 |
| e2 | 300 | 100 | 316.2 |
| bb* | 0 | 350 | 350.0 |

* No. bb was placed at the bottom of the bucket

When explosives were detonated at a scheduled acceleration level, a crater would be created in the standard sand. At the same time, the accelerometers recorded the acceleration response. The rotational speed of the centrifuge was reduced until it stopped. The craters were measured using a special vernier caliper. The measurement technique was achieved by placement of the vernier endpoint of contact with the sand surface. The accuracy of crater profile measurements along a given radial at 10 or 20 mm interval is within ±0.02 mm in the vertical direction.

## 3 Results and discussion

### 3.1 Crater dimensions

Fig. 3 shows the pictures of sand motion and a typical crater, which were taken by camera. Fig. 3a was recorded at the moment of sand splash, indicating that the sand was thrown up when the explosion occurred. Fig. 3b shows a typical crater. This crater was formed after the splashed sand fell back. It is known as an apparent crater that was measured along the dotted line in Fig. 3b.

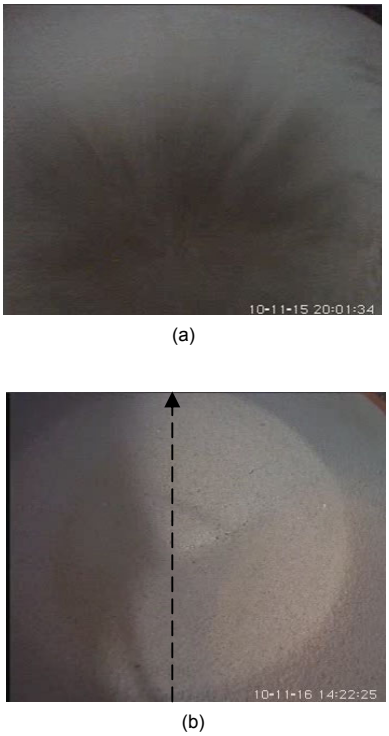


**Fig. 3 Pictures of sand motion (a) and a typical crater (b)**

The shapes of the ten apparent craters, depicted as half profiles in a representative radial direction, are shown in Fig. 4, respectively. Fig. 4a shows the four test results with 1 g of charge at 100 mm depth of burst when the acceleration level was increased from *g* to 100*g*. Fig. 4b shows three test results with 3 g of charge at 100 mm depth of burst when the acceleration level was increased from 40*g* to 100*g*. Fig. 4c shows three test results with 3 g of charge at 150 mm when the acceleration was increased from 40*g* to 100*g*. We can find that when the acceleration level is increased, the craters are less deep.

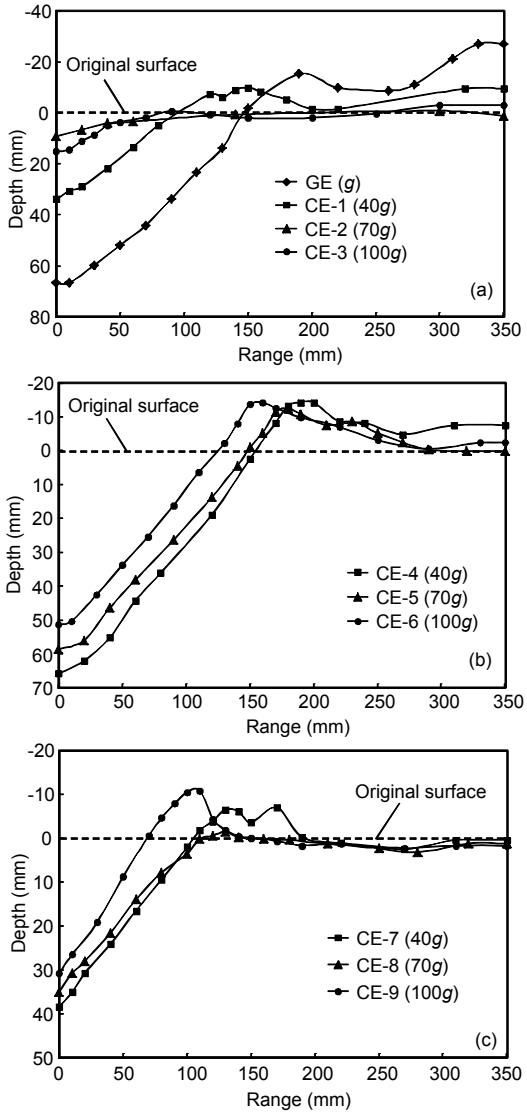


**Fig. 4 Apparent crater half profiles in 1 g of charge, 100 mm depth of burst (a), 3 g of charge, 100 mm depth of burst (b), and 3 g of charge, 150 mm depth of burst (c)**

In Fig. 4a, the craters of tests CE-2 and CE-3 are abnormally small because its energy involved in 1 g of charge cannot create an obvious crater at 70*g* and 100*g* acceleration levels.

Fig. 4 is also used to calculate the apparent crater volume below the original ground surface. Table 4 summarizes the apparent crater volumes, the test conditions, final crater dimensions and the values of the $\pi$ groups (Schmidt and Holsapple, 1980).

The $\pi$ groups are dimensionless parameters derived by similar analyses. Schmidt and Holsapple (1980) considered that the crater volume $V$ depends on seven parameters.

$$V = F\left(G, d, \delta, Y, \rho, a, Q\right), \tag{1}$$

where $G$ is the acceleration level, $d$ is the depth of burst, $\delta$ is the initial density of the explosive, $Y$ is the target material strength parameter, $\rho$ is the initial density of the target material, $a$ is the explosive charge radius, and $Q$ is the energy per unit mass of explosive. The charge mass $W$ can be calculated by

$$W = \frac{4}{3}\pi\delta a^3. \tag{2}$$

Eq. (1) can be rewritten in terms of the five $\pi$ groups:

$$\pi_1 = F(\pi_2, \pi_3, \pi_4, \pi_5), \tag{3}$$

where

$$\pi_1 = \frac{\rho V}{W}, \tag{4}$$

$$\pi_2 = \frac{G}{Q}\left(\frac{W}{\delta}\right)^{1/3}, \tag{5}$$

$$\pi_3 = d\left(\frac{\delta}{W}\right)^{1/3}, \tag{6}$$

$$\pi_4 = \frac{\rho}{\delta}, \tag{7}$$

$$\pi_5 = \frac{Y}{\delta Q}. \tag{8}$$

If the experiments are conducted in the same sand with the same explosive, $\pi_5$ is a constant, $\pi_3$ and $\pi_4$ can be denoted by $d/a$ and $\rho$, respectively. In

**Table 4 Cratering data summary***

| Test No. | $\rho$ (kg/m$^3$) | $W$ (g) | $a$ (mm) | $d$ (mm) | $G$ ($\times g$) | $V$ (m$^3$) | $\pi_2$ | $\pi_V$ |
|---|---|---|---|---|---|---|---|---|
| GE | $1.58\times10^3$ | 1 | 5.11 | 100 | 1 | $2.2965\times10^{-3}$ | $1.39\times10^{-8}$ | 3622.01 |
| CE-1 | $1.58\times10^3$ | 1 | 5.11 | 100 | 40 | $3.3625\times10^{-4}$ | $5.55\times10^{-7}$ | 530.34 |
| CE-2 | $1.58\times10^3$ | 1 | 5.11 | 100 | 70 | $1.0538\times10^{-4}$ | $9.71\times10^{-7}$ | 165.39 |
| CE-3 | $1.58\times10^3$ | 1 | 5.11 | 100 | 100 | $8.2990\times10^{-5}$ | $1.39\times10^{-6}$ | 130.37 |
| CE-4 | $1.58\times10^3$ | 3 | 7.37 | 100 | 40 | $1.9035\times10^{-3}$ | $8.01\times10^{-7}$ | 1003.98 |
| CE-5 | $1.58\times10^3$ | 3 | 7.37 | 100 | 70 | $1.4744\times10^{-3}$ | $1.40\times10^{-6}$ | 776.23 |
| CE-6 | $1.58\times10^3$ | 3 | 7.37 | 100 | 100 | $9.5188\times10^{-4}$ | $2.00\times10^{-6}$ | 503.64 |
| CE-7 | $1.46\times10^3$ | 3 | 7.37 | 150 | 40 | $6.6374\times10^{-4}$ | $8.01\times10^{-7}$ | 322.43 |
| CE-8 | $1.46\times10^3$ | 3 | 7.37 | 150 | 70 | $5.3881\times10^{-4}$ | $1.40\times10^{-6}$ | 262.88 |
| CE-9 | $1.46\times10^3$ | 3 | 7.37 | 150 | 100 | $2.7983\times10^{-4}$ | $2.00\times10^{-6}$ | 137.45 |

* For all the tests, $\delta$=1.786×10$^3$ kg/m$^3$ and $Q$=5.82×10$^6$ m$^2$/s$^2$

Eq. (4), only $V$ is unknown. Thus, $\pi_1$ is denoted by $\pi_V$. $\pi_V=\pi_1=\rho V/W$ is the ratio of thrown sand mass to explosive mass, consequently $\pi_V$ is also called cratering efficiency.

Eq. (5) can be rewritten as

$$\pi_2=\frac{(G^3W)^{1/3}}{Q\delta^{1/3}}, \tag{9}$$

where $G^3W$ is the equivalent charge when explosive fired at a high acceleration level. Here, $\pi_2$ is called gravity scaled yield.

Fig. 5 shows the relationship between $\pi_V$ and $\pi_2$. The results of the ten tests are divided into three groups based on the value of $d/a$. Each group is fitted to a straight line in the dual-logarithm coordinate system. The relationship between $\pi_V$ and $\pi_2$ is a power regression as

$$\pi_V\pi_2^{\alpha}=k_V=\text{const}, \tag{10}$$

where $\alpha$ and $k_V$ are constants depending on $d/a$ and $\rho$. For line No. 1, $d/a$=19.6 and $\rho$=1.58×10$^3$ kg/m$^3$:

$$\pi_V\pi_2^{0.69}=0.014. \tag{11}$$

For line No. 2, $d/a$=13.6 and $\rho$=1.58×10$^3$ kg/m$^3$:

$$\pi_V\pi_2^{0.72}=0.038. \tag{12}$$

For line No. 3, $d/a$=20.3 and $\rho$=1.46×10$^3$ kg/m$^3$:

$$\pi_V\pi_2^{0.88}=0.001. \tag{13}$$

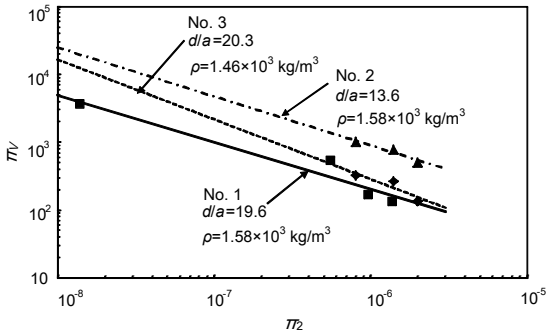


**Fig. 5 Cratering efficiency vs. gravity scaled yield**

Fig. 6 shows the results of GE, CE-1, CE-2, and CE-3 compared with previous studies (Schmidt *et al.*, 1986; Kutter *et al.*, 1988). The lines obtained by Schmidt *et al.* (1986) and Kutter *et al.* (1988) are close. Correspondingly, the cratering efficiency measured in this study is smaller than theirs. This can be explained by the differences in $d/a$, $\rho$ and the type of sand. Taking their approximate values of $d/a$ and $\rho$ into account, the results are acceptable.

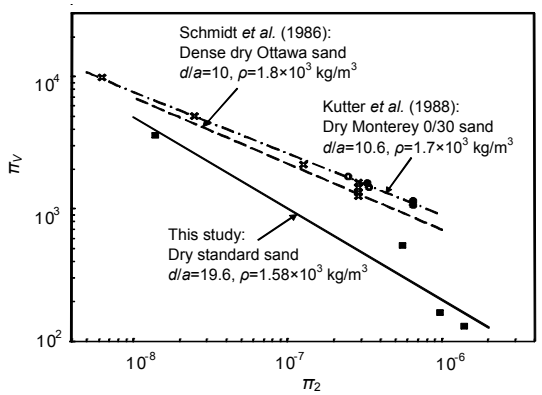


**Fig. 6 Comparison of results of this study and previous studies (Schmidt *et al.*, 1986; Kutter *et al.*, 1988)**

Schmidt (1977) used $\pi_1$, $\pi_2$ and $\pi_3$ to analyze charges buried in artist modeling clay. Through the combination of $\pi$ terms, a scaling law for crater volume in terms of the depth of charge burial was derived:

$$\pi_1\pi_2^{1/4} = F(\pi_3\pi_2^{1/6}). \quad (14)$$

Eq. (14) is used to fit the results of ten model tests as shown in Fig. 7.

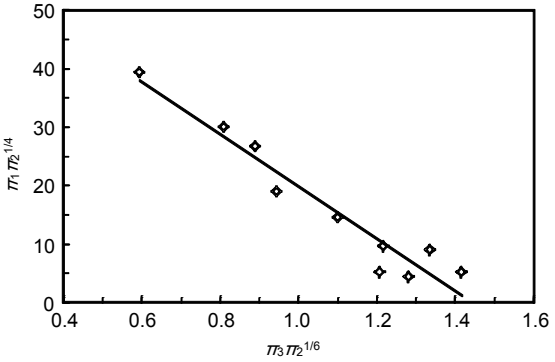


**Fig. 7 $\pi_1\pi_2^{1/4}$ vs. $\pi_3\pi_2^{1/6}$ in sand**

The relationship between $\pi_1\pi_2^{1/4}$ and $\pi_3\pi_2^{1/6}$ is approximately linear as follows:

$$\pi_1\pi_2^{1/4} = -44.669\pi_3\pi_2^{1/6} + 64.523,\ R^2=0.931. \quad (15)$$

Compared with Fig. 5, Fig. 7 is more applicable because of its simple formation and relatively high accuracy. Eq. (15) can be used to predict the crater volume if the attributes of sands and explosives are given.

### 3.2 Records of accelerations and discussions

The result from accelerometer No. c1 in test CE-6 indicated a pulse with 1250*g* peak acceleration as shown in Fig. 8. These accelerometers range from −2000*g* to 2000*g*, but at the position near explosive, the peak acceleration is invariably out of range, as can be seen from the records of accelerometers No. a1 and No. a2.

Fan *et al*. (2012) gave the valid peak accelerations recorded by the 11 accelerometers in the ten tests. Fig. 9 shows that the relationship between the proportional peak acceleration and proportional distance bears a power law relationship.

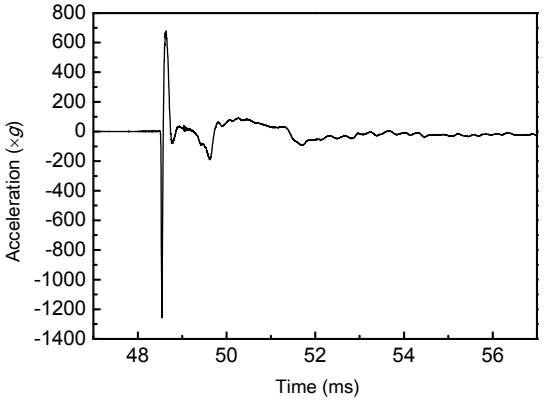


**Fig. 8 A typical blast wave (Fan *et al*., 2012)**

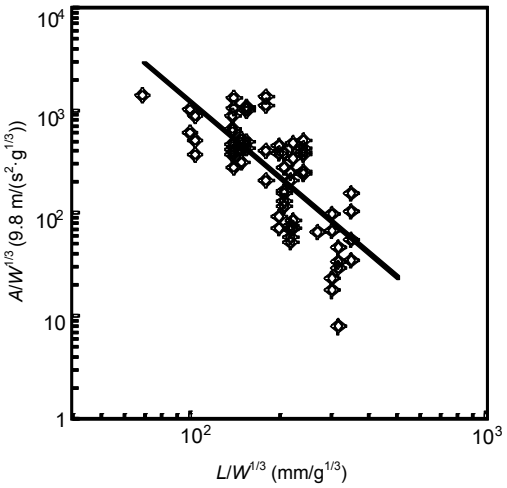


**Fig. 9 Curve of peak acceleration vs. proportional distance (Fan *et al*., 2012)**

*A* is the value of peak acceleration, and *L* is the distance from accelerometer to explosive

Fig. 10 shows that the proportional peak acceleration is a power increasing function of the gravity scaled yield at a certain distance. The proportional peak acceleration decreases as the distance increases when gravity scaled yield is a constant.

The acceleration wave in Fig. 8 presents important information about arrival time of the blast wave. The point that exhibits sharply turning trench at the very uneven line from the balance station is associated with the arrival time of blast waves. Fig.11 shows the curve of arrival time in each test. The curve of arrival time can be used to calculate the propagation velocity of blast waves traveling through sands. The velocity of blast waves is in the range of 200–714 m/s. The different accelerations result in different

sand densities, and then make the differences in propagation velocities.

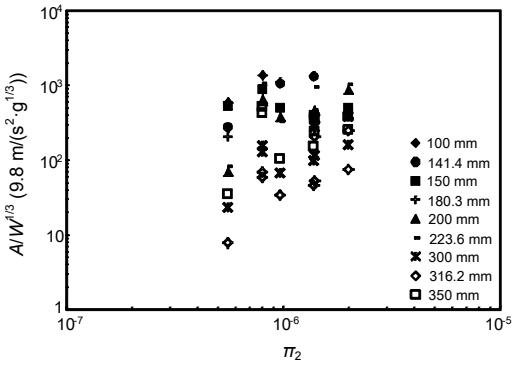


**Fig. 10 Curve of peak acceleration vs. gravity scaled yield (Fan *et al*., 2012)**

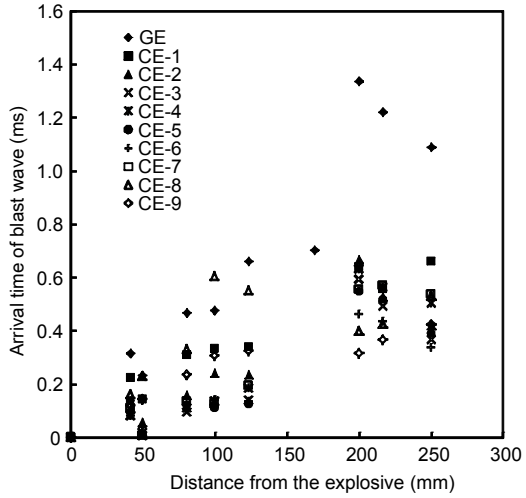


**Fig. 11 Curve of arrival time of blast wave**

## 4 Illustrative examples for applications

Two illustrative examples that are concerned with the materials of fuse-plug dams and lunar soils are presented. The gradations of these materials are considered to be close to those used in the experiments described in this study.

### 4.1 Example 1: Predicting dimensions of the crater in a fuse-plug dam

A fuse-plug dam with the sand density of $1.78\times10^3$ kg/m$^3$ is designed to be demolished by blasting. A 50 kg of RDX is assumed to be buried 1 m depth at the axis of dam. The progress of calculation can be given as

$$\pi_2=\frac{G}{Q}\left(\frac{W}{\delta}\right)^{1/3}=\frac{9.8}{5.82\times10^6}\times\left(\frac{50}{1.786\times10^3}\right)^{1/3}=5.113\times10^{-7}, \tag{16}$$

$$\pi_3=d\left(\frac{\delta}{W}\right)^{1/3}=1\times\left(\frac{1.786\times10^3}{50}\right)^{1/3}=3.293. \tag{17}$$

$\pi_1$ can be calculated by substituting Eqs. (16) and (17) into Eq. (15):

$$\pi_1=\frac{-44.669\pi_3\pi_2^{1/6}+64.523}{\pi_2^{1/4}}=\frac{-44.669\times3.293\times(5.113\times10^{-7})^{1/6}+64.523}{(5.113\times10^{-7})^{1/4}}=1920.998. \tag{18}$$

The volume of the crater can be predicted by substituting Eq. (18) into Eq. (4)

$$V=\frac{\pi_1 W}{\rho}=\frac{1920.998\times50}{1.78\times10^3}=53.96\ (\mathrm{m}^3). \tag{19}$$

The calculation results show that the explosion will tear a breach with about 53.96 m$^3$ in the fuse-plug dam. Then a reservoir water level higher than the bottom of the crater may cause a dam breach.

### 4.2 Example 2: Predicting dimensions of the crater on the moon

In the future, explosives might be used to establish shelter and mine on the moon. The lunar gravity is 0.17*g*. The density of lunar regolith is ranged between $1.30\times10^3$ to $2.29\times10^3$ kg/m$^3$ (Carrier *et al.*, 1991). An average value of $1.80\times10^3$ kg/m$^3$ is taken into calculation. A 15 kg of RDX is assumed to be buried 0.3 m depth in lunar regolith.

$$\pi_2=\frac{G}{Q}\left(\frac{W}{\delta}\right)^{1/3}=\frac{0.17\times9.8}{5.82\times10^6}\times\left(\frac{15}{1.786\times10^3}\right)^{1/3}=5.819\times10^{-8}, \tag{20}$$

$$\pi_3=d\left(\frac{\delta}{W}\right)^{1/3}=0.3\times\left(\frac{1.786\times10^3}{15}\right)^{1/3}=1.476. \tag{21}$$

$\pi_1$ can be calculated by substituting Eqs. (20) and (21) into Eq. (15):

$$\pi_1 = \frac{-44.669\pi_3\pi_2^{1/6} + 64.523}{\pi_2^{1/4}} = \frac{-44.669 \times 1.476 \times (5.819 \times 10^{-8})^{1/6} + 64.523}{(5.819 \times 10^{-8})^{1/4}} \quad (22)$$

$$=3890.173.$$

The volume of the crater can be predicted by substituting Eq. (22) into Eq. (4):

$$V = \frac{\pi_1 W}{\rho} = \frac{3890.173 \times 15}{1.80 \times 10^3} = 32.42\ (\mathrm{m}^3). \quad (23)$$

The results show that the explosion will create a crater with the volume of 32.42 $m^3$ in the lunar regolith.

The prediction of the two examples is shown in Fig. 12 by solid circle and hollow circle, respectively.

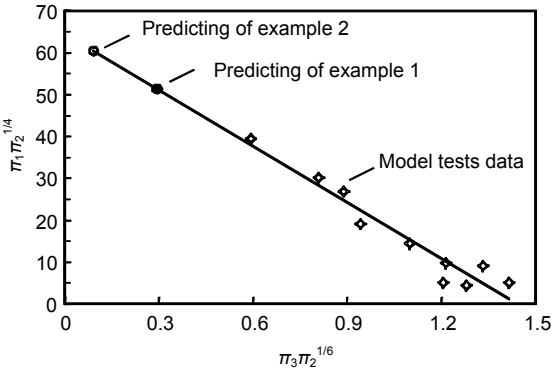


**Fig. 12 Predicting of the two examples by Eq. (15)**

## 5 Conclusions

Ten tests of explosion in sand were conducted through the 450 *g*-t centrifuge at IWHR to investigate the explosion catering effect and the propagation laws of blast wave. The following conclusions can be drawn.

1. The relationship between cratering efficiency $\pi_V$ and gravity scaled yield $\pi_2$ bears a power law $\pi_V \pi_2^{\alpha} = k_V = \text{const}$. The values of $\alpha$ and $k_V$ have been measured in the tests, associated with some typical values of $d/a$ and $\rho$. The cratering efficiency measured in this study is compared to that obtained by other studies with reasonable agreements. A scaling law that based on the combination of $\pi$ terms is given as

$$\pi_1\pi_2^{1/4} = -44.669\pi_3\pi_2^{1/6} + 64.523,\ R^2 = 0.931.$$

The relationship can be conveniently used to predict the cratering effects in sand.

2. The peak acceleration is a power increasing function of the gravity. The proportional peak acceleration is a power regression function of the proportional distance. In dry standard sand the propagation velocity of blast waves is in a range of 200 to 714 m/s in these ten tests.

Some conditions that may affect the results of a centrifuge test, for example, the atmospheric pressure, are not considered in Eq. (15), but the error is possibly appreciable. These limitations will be improved by further studies.

## Acknowledgements

The authors would like to thank the following colleagues and acknowledge their constructive advices and assistances: Drs. Yu-jing HOU, Ze-ping XU of IWHR, and Qiu-sheng WANG of Beijing University of Technology, who shared their experiences on experimental techniques and design; the engineers of IWHR centrifuge laboratory, Jian-hui LIANG, Xian-hui SONG and Jun-ming WU, who provided laboratory support.

## References

Carrier, W.D., Olhoetf, G.R., Mendell, W., 1991. Physical properties of the lunar surface. *In*: Heiken, G.H., Vaniman, D.T., French, B.M. (Eds.), Lunar Source Book. Cambridge University Press, New York, p.475-594.

Craig, W.H., 1989. Edouard Phillips (1821–1889) and the idea of centrifuge modeling. *Geotechnique*, **39**(4):697-700. [doi:10.1680/geot.1989.39.4.697]

Fan, Y.K., Liang, X.Q., Huang, X., Zhang, X.D., 2012. Blast wave effect on apparatus and propagation laws in dry sand in geotechnical centrifuge model tests. *Applied Mechanics and Materials*, **105-107**:626-629. [doi:10.4028/www.scientific.net/AMM.105-107.626]

Holsapple, K.A., Schmidt, R.M., 1979. A Material-Strength Model for Apparent Crater Volume. Proceedings of the 10th Lunar and Planetary Science Conference, Pergamon, New York, p.2757-2777.

Holsapple, K.A., Schmidt, R.M., 1987. Point-source solutions and coupling parameters in cratering mechanics. *Journal of Geophysical Research*, **92**(B7):6350-6376. [doi:10.1029/JB092iB07p06350]

Housen, K.R., Holsapple, K.A., 2003. Impact cratering on porous asteroids. *Icarus*, **163**(1):102-119. [doi:10.1016/S0019-1035(03)00024-1]

Housen, K.R., Holsapple, K.A., 2011. Ejecta from impact craters. *Icarus*, **211**(1):856-875. [doi:10.1016/j.icarus.2010.09.017]

Housen, K.R., Schmidt, R.M., Holsapple, K.A., 1983. Crater ejecta scaling laws: Fundamental forms based upon dimensional analysis. *Journal of Geophysical Research*, **88**(B3):2485-2499. [doi:10.1029/JB088iB03p02485]

JTJ051-93. Test Methods of Soils for Highway Engineering. China Communications Press, Beijing (in Chinese).

JTJ059-95. Field Test Methods of Subgrade and Pavement for Highway Engineering. China Communications Press, Beijing (in Chinese).

Kutter, B.L., O'Leary, L.M., Thompson, P.Y., Lather, R., 1988. Gravity-scaled tests on blast-induced soil-structure interaction. *Journal of the Geotechnical Engineering*, **114**(4):431-447. [doi:10.1061/(ASCE)0733-9410(1988)114:4(431)]

Lin, C.P., Goodings, D.J., Bernold, L.E., Dick, R.D., 1994. Modeling studies of effects on lunar soil of chemical explosions. *Journal of the Geotechnical Engineering*, **120**(10):1684-1703. [doi:10.1061/(ASCE)0733-9410(1994)120:10(1684)]

Ma, L.Q., Zhang, J.M., Hu, Y., Zhang, L.M., 2010. Centrifugal model tests for responses of shallow-buried underground structures under surface blasting. *Chinese Journal of Rock Mechanics and Engineering*, **29**(S2):3672-3678 (in Chinese).

Piekutowski, A.J., 1980. Formation of Bowl-Shaped Crater. Proceedings of the 11th Lunar and Planetary Science Conference, Pergamon, New York, p.2129-2144.

Pokrovsky, G.I., Fyodorov, I.S., 1965. Impact and Explosion Effects in a Deformable Medium. Liu, Q.R., Huang, W.B., translators. China Industry Press, Beijing (in Chinese).

Pokrovsky, G.I., Fyodorov, I.S., 1969. Centrifugal Model Testing in the Construction Industry. Niedra Publishing House, Moscow, Vols. I and II.

Schmidt, R.M., 1977. A Centrifuge Cratering Experiment: Development of a Gravity-Scaled Yield Parameter. Proceedings of the Symposium on Planetary Cratering Mechanics, New York, Pergamon Press, p.1261-1278.

Schmidt, R.M., Holsapple, K.A., 1980. Theory and experiments on centrifuge cratering. *Journal of Geophysical Research*, **85**(B1):235-252. [doi:10.1029/JB085iB01p00235]

Schmidt, R.M., Housen, K.R., 1987. Some recent advances in the scaling of impact and explosion cratering. *International Journal of Impact Engineering*, **5**(1-4):543-560. [doi:10.1016/0734-743X(87)90069-8]

Schmidt, R.M., Holsapple, K.A., Housen, K.R., 1986. Gravity Effects and Cratering. Report Prepared under Contract DNA-001-82-C-0301, Defense Nuclear Agency, Washington DC.

Simpson, P.T., Sausville, M.J., Zimmie, T.F., Abdoun, T.H., 2005. Geotechnical Centrifuge Modeling of Explosive Cratering on Earth Embankments and Dams. International Conference on Energy, Environment and Disasters (INCEED), Charlotte, North Carolina, USA, p.123-124.

Taylor, R.N., 1995. Geotechnical Centrifuge Technology. Blackie Academic and Professional, London.